

Bispecific antibodies targeting tumor-associated antigens and neutralizing complement regulators increase the efficacy of antibody-based immunotherapy in mice

P Macor¹, E Secco¹, N Mezzaroba¹, S Zorzet¹, P Durigutto¹, T Gaiotto², L De Maso¹, S Biffi³, C Garrovo³, S Capolla¹, C Tripodo⁴, V Gattei⁵, R Marzari¹, F Tedesco⁶ and D Sblattero⁷

The efficacy of antibody-based immunotherapy is due to the activation of apoptosis, the engagement of antibody-dependent cellular cytotoxicity and complement-dependent cytotoxicity (CDC). We developed a novel strategy to enhance CDC using bispecific antibodies (bsAbs) that neutralize the C-regulators CD55 and CD59 to enhance C-mediated functions. Two bsAbs (MB20/55 and MB20/59) were designed to recognize CD20 on one side. The other side neutralizes CD55 or CD59. Analysis of CDC revealed that bsAbs could kill 4–25 times more cells than anti-CD20 recombinant antibody in cell lines or cells isolated from patients with chronic lymphocytic leukemia. The pharmacokinetics of the bsAbs was evaluated in a human-SCID model of Burkitt lymphoma. The distribution profile of bsAbs mimics the data obtained by studying the pharmacokinetics of anti-CD20 antibodies, showing a peak in the tumor mass 3–4 days after injection. The treatment with bsAbs completely prevented the development of human/SCID lymphoma. The tumor growth was blocked by the activation of the C cascade and by the recruitment of macrophages, polymorphonuclear and natural killer cells. This strategy can easily be applied to the other anti-tumor C-fixing antibodies currently used in the clinic or tested in preclinical studies using the same vector with the appropriate modifications.

INTRODUCTION

Current strategies for cancer therapy with monoclonal antibodies (mAb) are mainly based on targeting proteins^{1–3} expressed on the surface of cancer cells that are easily accessible. Examples include the anti-Her2 Ab (trastuzumab) and the anti-EGF receptor Ab (cetuximab), which are used to treat solid tumors of the breast, head and neck, as well as colorectal cancers. Other successful applications include the anti-CD52 mAb (alemtuzumab) and anti-CD20 mAbs (rituximab, ofatumumab and obinutuzumab), which are currently being used in the treatment of hematological malignancies, such as leukemia and lymphoma.^{4,5} These antibodies exert anti-neoplastic effects either by inducing apoptosis^{6,7} or by engaging immune effector mechanisms, such as antibody-dependent cellular cytotoxicity (ADCC),^{8–10} antibody-dependent cellular phagocytosis¹¹ and complement-dependent cytotoxicity (CDC).^{12–14} The development of a novel strategy based on the use of bispecific antibodies (bsAbs) linking tumor cells with CD3 + T cells to increase cellular cytotoxicity represents a further advance in cancer therapy. The bsAbs have been constructed to simultaneously target both CD3 and several different tumor-specific antigens. The first approved antibody targeting CD19, catumaxomab,¹⁵ was followed by others that target Her2/neu, EGFR, CD66e, CD33, EphA2 and MCSP (or HMW-MAA).¹⁶ Both cytotoxic CD8 + T cells and CD4 + T cells can be redirected for tumor cell killing.^{17–19} Several other bsAbs are currently being tested in clinical trials. For example, blinatumomab, which is also known as MT103, targets CD3 and CD19. This antibody was tested in a Phase 1 trial in patients with

late-stage relapsed non-Hodgkin's lymphoma and in a Phase 2 trial in patients with B-precursor acute lymphoblastic leukemia.²⁰ MT110 is another bsAb targeting CD3 and epithelial cell adhesion molecule that has been tested in a Phase 1 trial in patients with lung and gastrointestinal cancer.²¹

Despite the advantages of the complement system (C) in the control of tumor growth, very few studies are based on bsAbs that enhance C-mediated functions.^{22,23} One advantage of the system is that it is made of soluble molecules that can easily reach the tumor site and diffuse inside the tumor mass.^{14,24,25} Moreover, C components are locally synthesized by many cell types, including macrophages,²⁶ fibroblasts²⁷ and endothelial cells^{28,29} and they are readily available as a first line of defense against cancer cells. However, a major limitation of C-mediated tumor cell lysis is the overexpression of the C-regulatory proteins CD46, CD55 and CD59 on the cell surface (mCRPs^{30,31}). These proteins permit evasion of complement attack and restricts the complement-dependent cytotoxic effect of several antibodies.¹⁴ Lysis of complement-resistant tumor cells is restored by the addition of antibodies neutralizing mCRPs, suggesting that the effect of mAbs can be enhanced by blocking their inhibitory activity.^{23,32,33} The *in vivo* use of these antibodies has been limited by the widespread distribution of the mCRPs on normal cells. Thus the only way to avoid undesirable attacks on host cells is to make the mCRP-neutralizing antibodies selectively target the cancer cells.³³

We now report the generation of two bsAbs that were designed to recognize CD20 and to neutralize the CD55 or CD59. The anti-CD20 antibody was selected as a prototype of a

¹Department of Life Sciences, University of Trieste, Trieste, Italy; ²National Institute for Biological Standards and Control (NIBSC), Hertfordshire, UK; ³Institute for Maternal and Child Health-IRCCS 'Burlo Garofolo', Trieste, Italy; ⁴Department of Human Pathology, University of Palermo, Palermo, Italy; ⁵Clinical and Experimental Onco-Hematology Unit, Centro di Riferimento Oncologico, I.R.C.C.S., Aviano, Italy; ⁶IRCCS Istituto Auxologico Italiano, Milan, Italy and ⁷Department of Health Sciences and IRCAD, University of Eastern Piedmont, Novara, Italy. Correspondence: Dr P Macor or Professor D Sblattero, Department of Life Sciences, University of Trieste, via Giorgeri, 5, Trieste 34127, Italy. E-mail: pmacor@units.it or sblatter@med.unipmn.it

therapeutic anti-tumor molecule able to cause C-dependent killing of cancer cells. The choice to neutralize CD55 and CD59 was based on our previous observations. We have demonstrated that these two C regulators contribute to the protection of CD20+ B-lymphoma cells from complement-mediated killing induced by rituximab³⁴⁻³⁶

Our data show that treatment with a mixture of the two bsAbs targeting CD20 on B-lymphoma cells prevents tumor development and results in the survival of all tumor-bearing animals.

MATERIALS AND METHODS

pDUO cloning procedures

The vector pMB-SV5³⁷ was used as a backbone for the construction of all plasmids used in this work. Two vectors were created for scFv cloning. The pMB407 vector was obtained by cloning a 759-bp fragment into the NheI-HindIII site of the PMB-SV5 vector. This fragment contained a codon-optimized sequence (Invitrogen, Milan, Italy) coding for the human immunoglobulin G1 (IgG1) Hinge_CH2-CH3 Fc region with the Y407T mutation, an SV5 tag, a furin cleavage site and the AgeI restriction site. The second vector, named pMB366, was obtained by cloning a 943-bp fragment containing a codon-optimized sequence coding for the AgeI restriction site and FMDV 2A sequence,³⁸ followed by the secretory leader sequence, BssHII-NheI restriction sites, the human IgG1 Hinge-CH2-CH3 Fc region with the T366Y mutation, and the 6xHis tag into the XbaI-HindIII site of the PMB-SV5 vector. The scFvs of interest were cloned into either the pMB366 or pMB407 vector as BssHII-NheI digested fragments. The final pDUO vector expressing the bispecific molecule was obtained by subcloning the scFv-Fc fragment that was cut from pMB366 with AgeI-HindIII restriction sites into a pM407 cut with the same enzymes. Anti-CD55 and CD59 scFvs were previously isolated³² and were subcloned into pMB407. The anti-CD20 scFv sequence was obtained on the basis of the amino-acid sequence of patent No. 5,736,137 (Idex Pharmaceuticals, San Diego, CA, USA). A fragment coding for the sequence-optimized VL linker VH was cloned in both pMB366 and pMB407 vectors. The fragment from pMB366 to pMB407 was subcloned into three different pDUO vectors to obtain coding regions for the bispecific molecules MB20/20, MB20/55 and MB20/59.

Antibodies and sera

The anti-CD20, anti-CD55 and anti-CD59 mAbs were obtained from ImmunoTools GmbH (Friesoythe, Germany). The anti-6xHis antibody was obtained from AbCam (Cambridge, UK) as was the mouse anti-SV5.³⁹ All the secondary antibodies were purchased from Sigma-Aldrich (Milan, Italy) or Aczon (Monte SanPietro, Bologna, Italy). The scFv-Fc were produced and purified from the supernatant of stably transfected CHO cells as previously described.⁴⁰

Normal human sera (NHS) from AB Rh+ blood donors were kindly provided by the Blood Transfusion Center (Trieste, Italy) and pooled as a source of complement.

Cells

The Burkitt lymphoma cell line BJAB, the B-chronic lymphocytic leukemia cell line MEC1 (a kind gift from Dr Josée Golay) and the ovarian carcinoma cell line IGROV1⁴¹ were grown in RPMI1640 medium (Sigma-Aldrich) supplemented with 10% fetal calf serum (Invitrogen). Heparinized peripheral blood samples were obtained after written informed consent from untreated B-CLL patients at the University Hospital in Trieste (B cells > 90% of total circulating cells). The study was approved by the IRB of the CRO (IRCCS) of Aviano (IRB-06-2010). The mononuclear cell fractions were isolated by centrifugation on Ficoll-Hypaque (GE Healthcare, Milan, Italy) density gradients.

Animals

Female SCID mice (4–6 weeks of age) were purchased from Charles-River (San Giovanni al Natissone, Udine, Italy) and maintained under pathogen-free conditions. All the experimental procedures were performed in compliance with the guidelines of the European (86/609/EEC) and the Italian (D.L.116/92) laws and were approved by the Italian Ministry of University and Research and the Administration of the University Animal House (Protocol 42/2012).

Enzyme-linked immunosorbent assay (ELISA)

Microtiter plate wells (Corning Life Sciences, Corning, NY, USA) were coated with 100 µl of solutions containing bsAbs by overnight incubation at 4 °C in 0.1 M of sodium bicarbonate buffer (pH 9.6), and the unbound sites were blocked by incubation with phosphate-buffered saline containing 2% skim milk for 1 h at 37 °C. The presence of antibodies was documented using anti-human IgG conjugated with alkaline phosphatase or using anti-SV5, anti-6xHis antibody and alkaline phosphatase-conjugated anti-mouse IgG. The enzymatic reaction was developed with PNPP (p-nitrophenyl phosphate) (Sigma-Aldrich; 1 mg/ml) as a substrate and read at 405 nm using Infinite M200Pro (TECAN ITALIA S.r.l., Cernusco sul Naviglio, Milano, Italy).

A sandwich ELISA was performed by binding anti-SV5 mAb on ELISA plates, and the binding of bsAbs was measured using horseradish peroxidase (HRP)-labeled anti-6xHis secondary antibody.

ELISA on cells

IGROV1 cells were grown to confluence in 96-well tissue culture plates (Corning Life Sciences). To evaluate cell-bound antibodies, the cells were incubated with 100 µl of primary antibodies diluted in phosphate-buffered saline containing 2% bovine serum albumin for 1 h at 37 °C. Then the cells were incubated with anti-SV5 or anti-6xHis mAbs and alkaline phosphatase-conjugated anti-mouse IgG. The enzymatic reactions were developed with PNPP and read at 405 nm.

Fluorescence-activated cell sorter (FACS) analysis

Lymphoma cells (5×10^5) were first incubated with the primary antibodies in phosphate-buffered saline containing 1% bovine serum albumin for 1 h at 37 °C and then with the appropriate fluorescein isothiocyanate-conjugated secondary antibodies for 1 h at 37 °C. The cells were fixed with 1% paraformaldehyde (Sigma-Aldrich), and the fluorescent signal was evaluated on a FACSCalibur instrument using the CellQuest software (BD Biosciences, San Jose, CA, USA).

Complement-mediated lysis

The previously described CDC procedure³³ was used to evaluate the effect of antibodies on the complement susceptibility of B-lymphoma and leukemia cells.

Mouse model of B-lymphoma

A xenograft B-lymphoma model was established in SCID mice to investigate the therapeutic effect of anti-CD20/20, anti-CD20/55 and anti-CD20/59. The animals were inoculated intraperitoneally (i.p.) on the right flank with 2×10^6 BJAB cells and examined twice weekly for up to 120 days for signs of sickness.⁴² Tissue samples from lymphoma-bearing mice were used for morphological, immunohistochemical or immunofluorescent analyses.

Evaluation of bsAb distribution using time-domain near-infrared optical imaging

Purified recombinant antibodies were labeled with the *N*-hydroxysuccinimide ester of Cy5.5 (FluoroLink Cy5.5 monofunctional dye; GE Healthcare). All the *in vivo* data were acquired using the small-animal time-domain Optix MX2 preclinical NIR-imager (Advanced Research Technologies, Montreal, CA, USA), as described by Biffi *et al.*^{43,44}

Immunofluorescence analysis

The tissue deposition of C components was previously described.³³ The presence of infiltrating natural killer cells (NK), macrophages (Mφ) and polymorphonuclear cells (PMN) was assessed in frozen sections (7 µm) of the tumor mass and other organs obtained from lymphoma-bearing mice at necropsy. The tissues were evaluated using rat mAbs to mouse CD56 (clone H28-123, Meridian Life Science, Cincinnati, OH, USA), to mouse Gr-1 (clone RB6-8C5, ImmunoTools) and polyclonal Ab to mouse CD14 (Santa Cruz, Dallas, TX, USA). The antibodies were incubated for 1 h at room temperature, followed by the relevant biotinylated secondary antibody (Dako, Glostrup, Denmark), and the staining was revealed with StreptABCComplex/HRP (Dako) and DAB + Chromogen (Dako).

Statistical analysis

The data were expressed as means \pm s.d. and analyzed by the two-tailed Student's *t*-test to compare two paired groups of data. The Kaplan–Meier product-limit method was used to estimate survival curves, and the log-rank test was adopted to compare different groups of mice.

RESULTS

Production of bsAbs

Our focus was to design and clone an expression construct to obtain stable and high-yield production of bsAbs using the 'knob-into-hole' mutations (Y407T and T366Y) in the human IgG CH3 domain. To this end, the selected scFvs were initially cloned individually into two different pMB366 and pMB407 vectors (Figure 1a) and then joined in the final vector pDUO (Figure 1b) to achieve expression and heterodimerization. This vector had the following features: (i) scFvs were fused to either the Y407T or T366Y mutated Fc region; (ii) each Fc region contained a C-terminal tag sequence for detection; and (iii) equal expression of both the scFv-Fc molecule chains was achieved with a single RNA molecule through the use of the FMDA 2A self-processing sequence. Furthermore, a furin-mediated cleavage site was included at the C-terminal end of the first tag (SV5) to remove the entire 2A peptide-tail. To achieve high-yield expression, all wild-type sequences were 'codon optimized' for expression in a CHO cell line.

Three different versions of the bispecific molecule were cloned. MB20/20 contained a scFv-Fc targeting CD20 on both arms.

The second and third bsAbs contained the scFv anti-CD20 fused to the T366Y-mutated Fc region and the scFv to CD55 or CD59 fused to the Y407T-mutated Fc portion. The result was the formation of bispecific molecules MB20/55 and MB20/59 (Figure 1c).

In vitro characterization of bsAbs

The three bsAbs were produced by stable transfection of CHO-S cells. The antibodies were affinity-purified using protein A columns,⁴⁰ and analysis was performed by sodium dodecyl sulfate-polyacrylamide gel electrophoresis (Supplementary Figure S1), western blotting (Figures 2a and b) and ELISA (Figure 2c). The results indicated the presence of a protein with the expected molecular weight of 115–120 kDa, which corresponds to the scFv-Fc dimers. Monomers, degradation products or other contaminating proteins were below the detection limits in all preparations.

Immunoenzymatic assays were used to address the important issue of heterodimer formation. We used the anti-6xHis mAb to document the presence of the anti-CD20 and the anti-SV5 mAb to reveal the presence of the other arm in the bispecific molecules (Figure 2b). Analysis of the purified proteins by a sandwich ELISA using anti-SV5 as a trapping mAb and HRP-labeled anti-6xHis mAb as a revealing reagent for the bound bsAbs showed the formation of heterodimers.

To investigate the cell-binding activity of the purified molecules, we first examined the binding of MB20/20, MB20/55 and MB20/59 to cancer B-cells by FACS analysis. This study confirmed that all

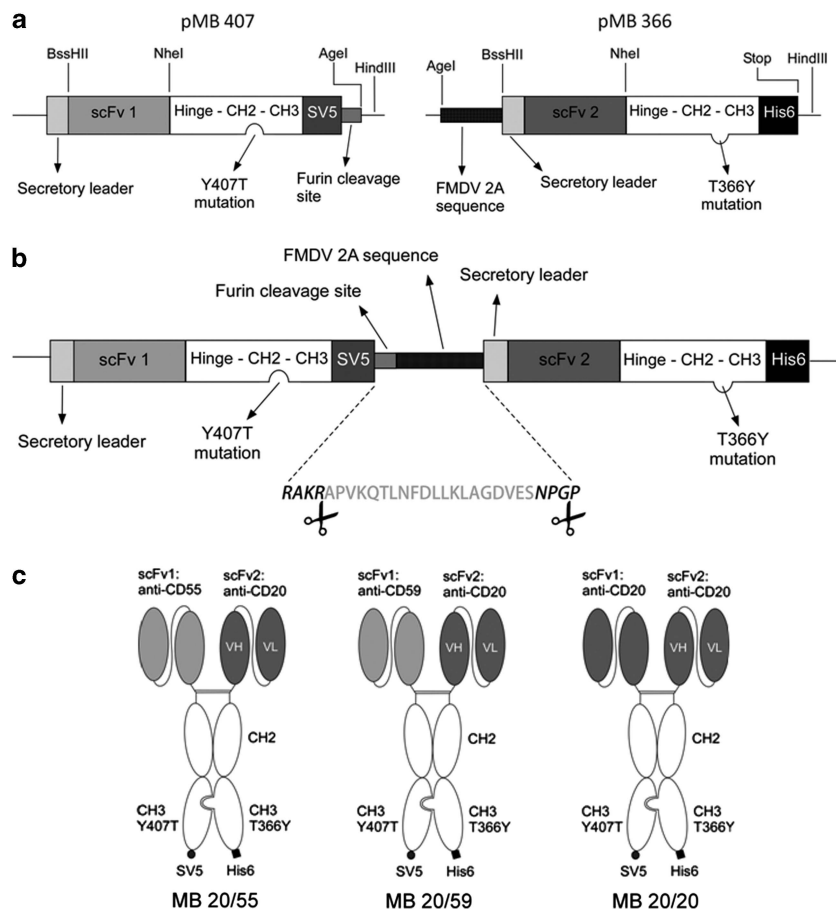


Figure 1. Schematic representation of the bsAbs expression vector. (a) scFv of interest are initially cloned into two different scFv-Fc expression vectors. pMB407 contains the Y407T mutation and the SV5 tag while pMB366 contains the T366Y mutation and the 6xHis tag. (b) The final pDUO vector expressing a bispecific molecule was obtained by subcloning the scFv-Fc fragment from pMB366 into a pMB407. The vector contains the FMDV2A sequence and a furin cleavage site between the two scFv-Fc to allow expression of two proteins from a single RNA. (c) Three different versions of the bispecific molecules produced MB20/55, MB20/59 and MB20/20.

three antibodies were able to bind to the BJAB lymphoma cell line expressing CD20, CD55 and CD59 (Figure 3). We have initially characterized the saturating concentration of bsAbs for binding to BJAB cells (10 μ g/ml) and used this condition for all the *in vitro* tests. When the mixture of MB20/55 and MB20/59 was used, the final antibody concentration was maintained at 10 μ g/ml using 5 μ g/ml of each molecule.

As the binding of the bsAbs to the cell surface can be mediated either by the anti-CD20 or the anti-mCRP arms, we used ELISA to analyze their binding to the epithelial ovarian carcinoma cell line IGROV1. This cell line expresses CD55 and CD59⁴¹ but not CD20. As expected, MB20/20 failed to interact with these cells, whereas MB20/55 and MB20/59 bsAbs maintained their ability to bind to tumor cells (Figure 3). BJAB cells were also preincubated with

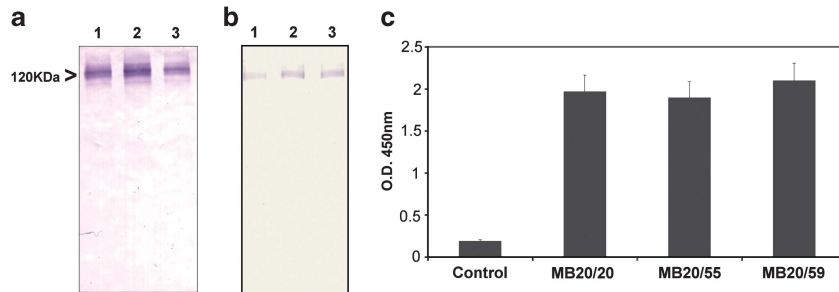


Figure 2. Production of bsAbs. MB20/20 (1), MB20/55 (2) and MB20/59 (3) production was documented by western blotting analysis using anti-SV5 (a) and anti-6xHis (b) mAbs. Heterodimer formation was evaluated by a sandwich ELISA using anti-SV5/anti-6xHis-HRP, as described in Material and methods (c).

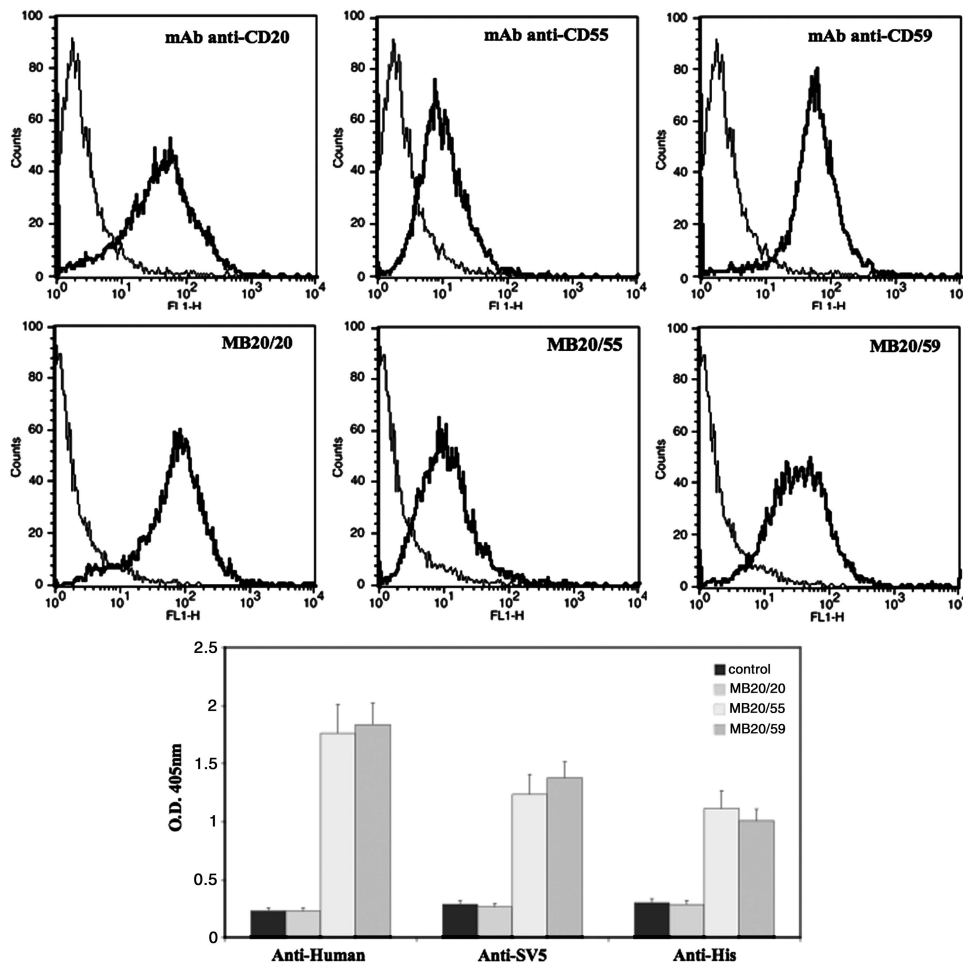


Figure 3. Binding of MB20/20, MB20/55 and MB20/59 to tumor cell lines. The expression of CD20, CD55 and CD59 on the BJAB cell line was investigated by FACS analysis using commercial antibodies (top row). Binding of bsAbs to BJAB cells was evaluated using anti-human fluorescein isothiocyanate-labeled secondary antibodies (middle row). Grey lines represent control Ab binding. Cell ELISA performed on ovarian carcinoma cells (IGROV1) not expressing CD20 to determine the binding of anti-CD55 and anti-CD59 (bottom row). The cells were incubated with bsAbs or control antibody and revealed using anti-human, anti-SV5 and anti-His secondary antibodies. Note the binding of MB20/55 and MB20/59 but not of MB20/20.

10 × more concentrated MB55 + MB59³³ in order to obtain CD20 + B-cells but shielded for CD55 and CD59. The binding of biotin-labeled BsAbs was measured by flow cytometry. The results presented as mean fluorescence intensity in Supplementary Table S1 clearly indicated that binding of bsAbs was not prevented by shielding the CD55 and CD59 epitopes. On the contrary, binding of MB20/55 and MB20/59 to BJAB cells was markedly reduced when the cells were preincubated with Rituximab.

The capacity of bsAbs to induce complement-mediated killing was tested using the Burkitt lymphoma cell line BJAB and the chronic lymphocytic leukemia cell line MEC1. The cells were exposed to recombinant antibodies and NHS (25%) as a source of complement for 1 h at 37°C. As shown in Table 1, the CDC obtained with MB20/20 was 15% for MEC1 and 22% for BJAB. Such low levels of cytotoxicity suggested that surface-expressed complement regulators may account for the resistance of these cells to complement attack. Because CD55 and CD59 were previously found to be responsible for cell protection from CDC,^{32,33,35} the cells were incubated with NHS in the presence of MB20/55, MB20/59 or the mixture of both bsAbs. The results presented in Table 1 show that the percentage of cells killed increased considerably following the neutralization of mCRPs. In particular, the CDC induced by the mixture of bsAbs was up to threefold higher than that obtained with MB20/20.

To prove that MB20/55 and MB20/59 selectively target B-cells, BJAB cells were incubated with bsAbs and serum in the presence of either human red cells (40% v/v) or T cells (2×10^5) expressing CD55 and CD59. Despite the high number of erythrocytes or T cells, the complement-dependent killing of BJAB cells exceeded 50% and attained a value that was not significantly different from the result obtained in the absence of bystander cells (Supplementary Figure S2).

The ability of an antibody to activate the classical pathway of the complement system depends on the level of antibody deposited on the cell surface and on the amount of tumor-associated antigen. BJAB and MEC1 cells express high levels of CD20. High CD20 expression is uncommon in B-lymphoproliferative disorders such as chronic lymphocytic leukemia (CLL), which is characterized by low levels of CD20 on circulating tumor B-cells. Therefore, we decided to compare the killing of B-cell lines induced by saturating concentration of recombinant Abs with the CDC of cells isolated from patients with CLL that express low levels of CD20 (Table 1). MB20/20 was able to kill <10% of patient's cells but the killing effect of the antibody increased substantially by blocking CD55 or CD59 with MB20/55 and MB20/59 antibodies. The results showed an enhanced CDC of 33% and 38%, respectively. The cell cytotoxicity reached 58% when a mixture of MB20/55 and MB20/59 was used at the same final concentration of antibodies (Table 1; * $P < 0.01$ vs MB20/20-treated cells).

In vivo characterization of bsAbs

To ascertain whether the mixture of MB20/55 and MB20/59 maintained a synergistic effect *in vivo*, BJAB cells were injected

i.p. into SCID mice. This resulted in the development of a lymphoma model that led to the animal death in 50–70 days after cell inoculation. Peritoneal tumor masses were observed in all mice at necropsy, with the histological appearance of aggregates of lymphoid cells positive for human CD20. Foci of lymphoid cells were observed in the liver, bone marrow and spleen. The *in vivo* distribution of the bsAbs was monitored by labeling the molecules with near-infrared dye and injecting them i.p. into tumor-bearing mice. The bsAbs were monitored using time-domain optical imaging. The whole-body scans shown in Figure 4a revealed a strong fluorescence signal in the region of probe injection, but the signal decreased exponentially and remained restricted to a limited area. This finding is consistent with the results obtained with other antibodies.⁴³ The fluorescence signal became evident in the tumor mass 4 h after injection and increased progressively during the next 4 days (Figure 4b). The accumulation curves of anti-CD20 and bsAbs were essentially similar, though the two bsAbs MB20/55 and MB20/59 reached the tumor mass faster than MB20/20. The peak for bsAbs MB20/55 and MB20/59 was 48 h, whereas MB20/20 peaked after 72 h (Figure 4c).

The ability of tissue-bound antibodies to activate the complement system was evaluated by analyzing the deposition of C3 and C9 in the tumor masses of animals receiving saline, MB20/20, MB20/55, MB20/59 or the mixture of the two bsAbs. Unlike the saline-treated groups, the animals treated with the anti-CD20 scFv-Fc showed signs of complement activation based on massive deposition of C3 and mild C9 staining. The staining increased substantially in mice receiving the mixture of MB20/55 and MB20/59 (Figure 5a).

Activation of the complement system is known to stimulate the inflammatory process. Therefore we examined the tumor masses for the presence of PMN, Mφ and NK cells recruited into the tumor microenvironment as a result of complement activation. The PMN were barely detectable in the tumors of anti-CD20-, anti-CD20/55- and anti-CD20/59-treated mice. However, massive infiltration of these cells was observed in mice that received the combination of bsAbs. MB20/20, MB20/55 and MB20/59 administered individually recruited less Mφs than PMN, and a larger number of these cells were mobilized by the mixture of bsAbs. A strong NK infiltrate was observed in tumor masses collected from MB20/55 + MB20/59-treated animals, whereas a limited number of NK cells was found in mice receiving either MB20/55 or MB20/59 (Figure 5b). The histological analysis showed apoptotic/necrotic areas that were mainly present in tumor masses collected from animals treated with the mixture of bsAbs (Supplementary Figure S3).

Therapeutic effect of bsAbs

The *in vitro* and *in vivo* data showed that BJAB cells could efficiently be targeted and killed by bsAbs. To prove that these antibodies also had therapeutic effect, a human/mouse model of lymphoma was established in SCID mice that received an i.p. injection of BJAB cells. The mice were then treated with MB20/20, MB20/55 and MB20/59 administered either individually

Table 1. Complement-mediated killing of purified tumor B-cells

	CD20 (MFI)	CD55 (MFI)	CD59 (MFI)	Saline	MB20/20	MB20/55	MB20/59	MB20/55 + MB20/59
BJAB	316.8	12.0	92.2	3.1 ± 1.1	22.0 ± 1.9	31.3 ± 3.9*	38.3 ± 4.3*	57.8 ± 6.1*
MEC1	264.5	19.0	92.0	0.9 ± 1.3	15 ± 1.9	23.5 ± 3.8	33.4 ± 3.5*	44.1 ± 7.0*
Pt1	73.6	38.3	87.5	2.1 ± 1.4	1.3 ± 1.1	33.5 ± 4.5*	34.2 ± 5.1*	53.9 ± 10.8*
Pt2	22.2	6.3	63.0	1.4 ± 1.4	1.4 ± 1.0	10.7 ± 3.8*	9.2 ± 2.8*	21.0 ± 5.7*
Pt3	65.9	13.3	67.9	4.3 ± 1.0	9.1 ± 2.1	19.5 ± 3.7*	19.7 ± 2.9*	43.8 ± 8.4*
Pt4	53.6	11.2	67.2	6.3 ± 1.8	9.9 ± 1.9	18.6 ± 2.1*	23.4 ± 4.3*	39.7 ± 8.3*
Pt5	77.7	27.4	91.0	1.2 ± 1.0	4.2 ± 2.0	31.4 ± 3.6*	38.7 ± 5.0*	57.6 ± 10.8*

Abbreviation: MFI, mean fluorescence intensity. * $P < 0.01$ vs MB20/20.

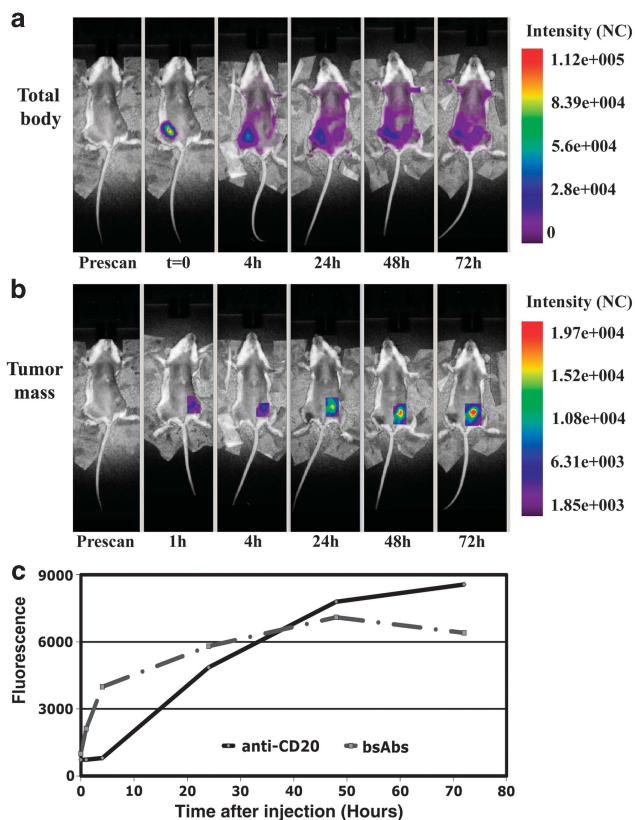


Figure 4. *In vivo* distribution of bispecific recombinant antibodies. Time-domain optical images of the total body (a) or the tumor mass (b) of representative tumor-bearing mice (3 animals) injected with anti-CD20 or bsAbs. The distribution of the labeled molecules was assessed at the indicated times over a period of 3 days. The distribution pattern was similar in all treated animals. Color bar is shown at the right for comparison. The average fluorescence intensity is indicated by the normalized counts (NC). The time course of fluorescence intensity in the tumor mass (c) is expressed as the average fluorescence intensity (NC) of a selected area localized over the tumor mass at the indicated time point.

or as a mixture. Fifty micrograms of recombinant antibodies were injected in each animal. The dose was reduced to 25 μ g in animals receiving the mixture of two bsAbs. The treatment was repeated twice on days 4 and 11, and the animals were followed up to 120 days. As shown in Figure 6, all the tumor-bearing mice receiving saline died within 60 days and survived slightly longer when treated with MB20/20. Mice treated with MB20/55 or MB20/59 had a significantly prolonged survival, with 80% of animals dying within 80 and 120 days, respectively, and 20% still alive at the end of the experiment ($P < 0.05$ vs saline or MB20/20-treated animals in a log-rank test). Interestingly, the combined treatment with MB20/55 and MB20/59 resulted in a synergistic effect leading to 100% survival of the animals ($P < 0.01$ vs bsAb). Tumors failed to develop in all the treated mice, and histological examination of the organs did not reveal the presence of residual human tumor B-cells.

DISCUSSION

BsAbs have been generated in recent years with the aim of bringing effector cells of the immune system into close contact with target cells to simultaneously engage tumor cell antigens and surface molecules on immune cells and facilitate their cytotoxic activity.¹⁶ Oncology dominates the field of bsAbs, and many drugs are in Phase I and II clinical trials or received approval for

marketing.²⁰ However, the relatively high number of effector cells required in the tumor microenvironment to cause cytotoxic damage to cancer cells represents the main limitation of this approach. The data presented here show that an alternative strategy to obtain an effective control of tumor growth can be offered by bsAbs that focus the effector function of the C system on tumor cells.

The anti-CD20 antibody rituximab, currently used to treat some B-cell malignancies and antibody-mediated autoimmune disorders, was selected as a prototype of a therapeutic anti-tumor molecule able to activate C and cause C-dependent killing of cancer cells. This antibody was combined with neutralizing antibodies to CD55 and CD59 to generate the bsAbs MB20/55 and MB20/59. The choice to neutralize these two mCRPs was based on our previous observation that B-lymphoma cells are protected from C attack, mainly by CD55 and CD59, with only a negligible contribution of CD46.^{34–36} This finding suggests that the mCRPs to neutralize *in vivo* should be selected on the basis of functional activity rather than on the degree of surface expression.

Successful heterodimerization is a critical issue for the production of active bispecific fragments containing an Fc region, because it confers long serum half-life and supports secondary immune functions, such as ADCC and CDC. The knobs-into-holes strategy based on the substitution of amino acids at the contact site between the CH3 domains of the human IgG1 Fc region was used to generate stable heterodimers, as suggested by the finding of scFv-Fc dimers in the supernatant of CHO-S secreting bsAbs. Additionally, we were not able to detect monomers or degradation products.⁴⁵ Furthermore, this format of bsAbs was engineered using a single polypeptide expression approach to ensure balanced production of both scFv-Fc chains. This goal was achieved by designing a vector that included a FMDV 2A self-cleaving peptide³⁸ in addition to a furin cleavage site.⁴⁶

The bsAbs MB20/55 and MB20/59 proved to be more effective than the parent molecule MB20/20 in inducing C-dependent cytotoxicity. The anti-CD20 antibody exhibited only a modest killing effect on B-cells from CLL patients that did not exceed 10%. This result is compatible with the low level of CD20 expressed by CLL B-cells.^{47–49} However, despite the limited number of CD20 molecules on the surface of these cells, the mixture of MB20/55 and MB20/59 caused a 4–25-fold increase in cell killing compared with MB20/20. These findings suggest that the evasion of cancer cells from C attack depends on the control of C activation by CD55 and CD59.

One problem with the potential clinical use of the bsAbs is their selective delivery to cancer cells, given the wide distribution of mCRPs on circulating and endothelial cells. These cells may absorb a large proportion of infused molecules and prevent their deposition on the tumor mass. Additionally, these cells may become exposed to C attack. Unfortunately, this issue could not be addressed using the *in vivo* model established in SCID mice, because the three antibodies only recognize the human targets and did not cross-react with the murine counterparts. To address this issue, we obtained data from the *in vitro* assay, which showed that the killing of the Burkitt lymphoma cell line BJAB remained essentially unchanged in the presence of a large number of erythrocytes or T cells. This result confirms that the targeting was driven by the MB20 high-affinity arm rather than from either anti-CD55 or anti-CD59 arm that have lower affinity for their respective target antigens.

The bsAbs injected *i.p.* into tumor-bearing SCID mice maintained their ability to target human cancer B-cells *in vivo*. The three antibodies had similar accumulation profiles that peaked at 48/72 h after injection. The administration of bsAbs represents a significant advance compared with the three-step biotin-avidin system previously used to deliver MB55 and MB59 to rituximab-coated tumor cells in a mouse model of B-lymphoma.³³ Although this therapeutic approach was successful, it has some major

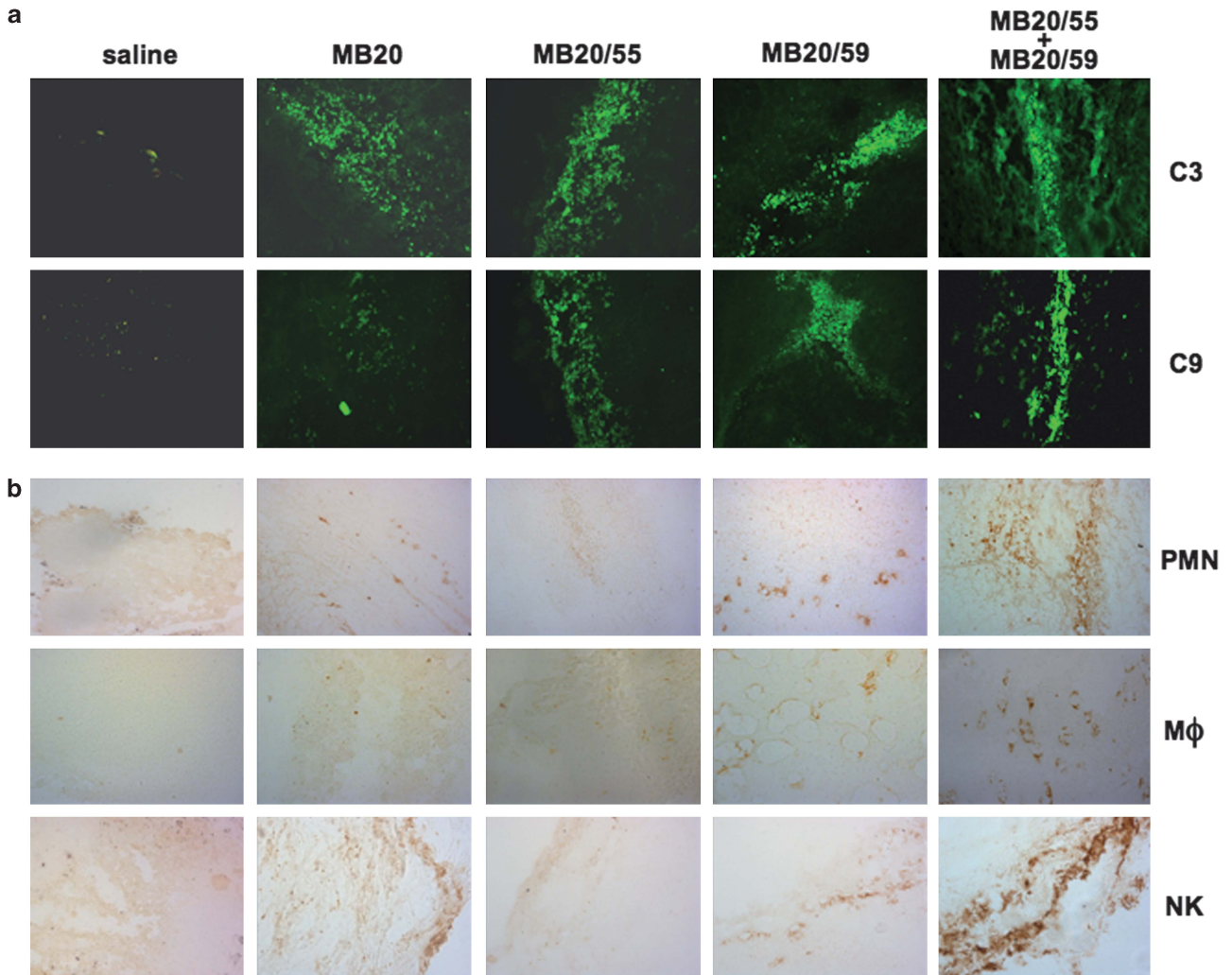


Figure 5. Immunofluorescence analysis of tumor masses from xenograft mice receiving saline, MB20/20, MB20/55, MB20/59 and MB20/55 + MB20/59. Deposition of complement components (a) and leukocyte recruitment (b) were analyzed using antibodies against C3, C9, GR1 (PMN), CD14 (Macrophages) and CD56 (NK cells). Saline-treated mice were used as a negative control group to show the absence of complement activation and leukocyte infiltration in untreated animals. Pictures were taken at $\times 200$ original magnification.

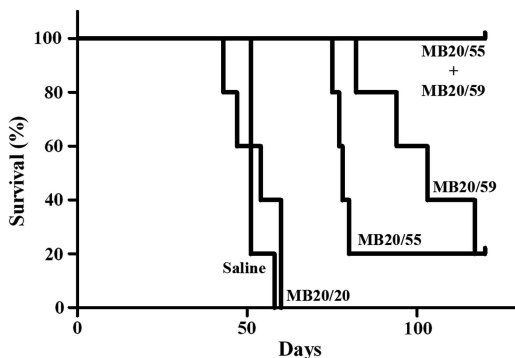


Figure 6. Effect of increasing doses of bispecific recombinant antibodies on survival of SCID mice challenged with BJAB cells. Mice were injected i.p. with BJAB cells and treated on days 4 and 11 with saline, MB20/20, MB20/55, MB20/59 or MB20/55 + MB20/59. Animals were followed up for 120 days, and survival was evaluated.

drawbacks, including the risk that the biotinylation procedure may impair the antibody function, the potential immunogenicity of avidin and the inconvenience caused to the patients by the separate infusions of two biotin-labeled antibodies and avidin.

The treatment of tumor-bearing mice with the combination of the two bsAbs was highly effective in controlling tumor growth and resulted in the survival of all the treated mice. The finding of massive deposition of C3 and particularly of C9 in the tumor mass of bsAbs-treated mice supports the involvement of the effector phase of C activation in tumor destruction. Strong C activation induced by the mixture of MB20/55 and MB20/59 may cause a direct cytotoxic effect through the membrane attack complex as suggested by the extensive damage of tumor cells observed in these animals. C can also contribute to control tumor growth by recruiting PMN cells, macrophages and NK cells through the release of C5a⁵⁰ and possibly by the soluble terminal complement complex.⁵¹ These cells exert cytotoxicity on tumor cells via ADCC and phagocytosis using the Fc portion of the bound antibodies and via C-dependent cell cytotoxicity using C3 fragments bound to the surface of tumor cells.

The effect of C5a on tumor progression is a controversial issue. The release of C5a in the tumor microenvironment was reported by Markiewski *et al.*⁵² to enhance tumor growth by recruiting myeloid-derived suppressor cells that suppress the anti-tumor CD8 + T-cell-mediated response. More recently, Gunn *et al.*⁵⁰ have shown that the effect of C5a depends on the level locally available. Using a human ovarian carcinoma xenograft model in mice, they

found that high C5a levels favor tumor growth and suppresses anti-tumor T-cell infiltration. However, a low level of C5a has the opposite effect. It is difficult to estimate the relevance of this finding in the clinical setting when using an anti-tumor antibody therapy because of the difficulty of assessing the level of C5a at the tumor site. However, our previous *in vitro* observation on the antibody-induced killing of ovarian carcinoma cell lines in the presence of neutralizing antibodies to mCRPs was mainly caused by complement-dependent lysis, and there was only a modest contribution of cell-mediated cytotoxicity.⁴¹

In conclusion, we have developed two novel therapeutic bsAbs that are able to target B-cells and to enhance tumor cell killing, both *in vitro* and *in vivo*. Although this approach was devised for the generation of bsAbs carrying the specificity of the anti-CD20 Ab rituximab, this strategy can easily be applied the other anti-tumor C-fixing antibodies currently used in the clinic or tested in preclinical studies using the same vector with the appropriate modifications.

CONFLICT OF INTEREST

The authors declare no conflict of interest.

ACKNOWLEDGEMENTS

This work was financially supported by Regione Friuli Venezia Giulia (Linfonet and AITT—to FT), the Italian Association for Cancer Research (AIRC Project no. 12965/2012—to PM), Fondazione Kathleen Foreman Casali—Trieste (to PM) and Fondazione Sanpaolo (to DS).

REFERENCES

- Baker M. Upping the ante on antibodies. *Nat Biotechnol* 2005; **23**: 1065–1072.
- Cohen J, Wilson A. New challenges to medicare beneficiary access to mAbs. *MAbs* 2009; **1**: 56–66.
- Ledford H. 'Biosimilar' drugs poised to penetrate market. *Nature* 2010; **468**: 18–19.
- Adams GP, Weiner LM. Monoclonal antibody therapy of cancer. *Nat Biotechnol* 2005; **23**: 1147–1157.
- Hong CW, Zeng Q. Awaiting a new era of cancer immunotherapy. *Cancer Res* 2012; **72**: 3715–3719.
- Byrd JC, Kitada S, Flinn IW, Aron JL, Pearson M, Lucas D *et al*. The mechanism of tumor cell clearance by rituximab *in vivo* in patients with B-cell chronic lymphocytic leukemia: evidence of caspase activation and apoptosis induction. *Blood* 2002; **99**: 1038–1043.
- Banerji R, Kitada S, Flinn IW, Pearson M, Young D, Reed JC *et al*. Apoptotic-regulatory and complement-protecting protein expression in chronic lymphocytic leukemia: relationship to *in vivo* rituximab resistance. *J Clin Oncol* 2003; **21**: 1466–1471.
- Hubert P, Amigorena S. Antibody-dependent cell cytotoxicity in monoclonal antibody-mediated tumor immunotherapy. *Oncoimmunology* 2012; **1**: 103–105.
- Nimmerjahn F, Ravetch JV. Fcγ receptors: old friends and new family members. *Immunity* 2006; **24**: 19–28.
- Weiner LM, Surana R, Wang S. Monoclonal antibodies: versatile platforms for cancer immunotherapy. *Nat Rev Immunol* 2010; **10**: 317–327.
- Winiarska M, Glodkowska-Mrowka E, Bil J, Golab J. Molecular mechanisms of the antitumor effects of anti-CD20 antibodies. *Front Biosci (Landmark Ed)* 2011; **16**: 277–306.
- Dunkelberger JR, Song WC. Complement and its role in innate and adaptive immune responses. *Cell Res* 2010; **20**: 34–50.
- Zipfel PF, Skerka C. Complement regulators and inhibitory proteins. *Nat Rev Immunol* 2009; **9**: 729–740.
- Macor P, Tedesco F. Complement as effector system in cancer immunotherapy. *Immunol Lett* 2007; **111**: 6–13.
- Maher J, Adami AA. Antitumor immunity: easy as 1, 2, 3 with monoclonal bispecific trifunctional antibodies? *Cancer Res* 2013; **73**: 5613–5617.
- Baeuerle PA, Reinhardt C. Bispecific T-cell engaging antibodies for cancer therapy. *Cancer Res* 2009; **69**: 4941–4944.
- Brischwein K, Parr L, Pflanz S, Volkland J, Lumsden J, Klinger M *et al*. Strictly target cell-dependent activation of T cells by bispecific single-chain antibody constructs of the BiTE class. *J Immunother* 2007; **30**: 798–807.
- Haas C, Krinner E, Brischwein K, Hoffmann P, Lutterbuse R, Schlereth B *et al*. Mode of cytotoxic action of T cell-engaging BiTE antibody MT110. *Immunobiology* 2009; **214**: 441–453.

- Baeuerle PA, Kufer P, Bargou R. BiTE: Teaching antibodies to engage T-cells for cancer therapy. *Curr Opin Mol Ther* 2009; **11**: 22–30.
- Klinger M, Brandl C, Zugmaier G, Hijazi Y, Bargou RC, Topp MS *et al*. Immunopharmacologic response of patients with B-lineage acute lymphoblastic leukemia to continuous infusion of T cell-engaging CD19/CD3-bispecific BiTE antibody blinatumomab. *Blood* 2012; **119**: 6226–6233.
- Maetzel D, Denzel S, Mack B, Canis M, Went P, Benk M *et al*. Nuclear signalling by tumour-associated antigen EpCAM. *Nat Cell Biol* 2009; **11**: 162–171.
- Blok VT, Daha MR, Tijmsma O, Harris CL, Morgan BP, Fleuren GJ *et al*. A bispecific monoclonal antibody directed against both the membrane-bound complement regulator CD55 and the renal tumor-associated antigen G250 enhances C3 deposition and tumor cell lysis by complement. *J Immunol* 1998; **160**: 3437–3443.
- Gelderman KA, Blok VT, Fleuren GJ, Gorter A. The inhibitory effect of CD46, CD55, and CD59 on complement activation after immunotherapeutic treatment of cervical carcinoma cells with monoclonal antibodies or bispecific monoclonal antibodies. *Lab Invest* 2002; **82**: 483–493.
- Klepfish A, Gilles L, Ioannis K, Rachmilewitz EA, Schattner A. Enhancing the action of rituximab in chronic lymphocytic leukemia by adding fresh frozen plasma: complement/rituximab interactions & clinical results in refractory CLL. *Ann NY Acad Sci* 2009; **1173**: 865–873.
- Klepfish A, Rachmilewitz EA, Kotsianidis I, Patchenko P, Schattner A. Adding fresh frozen plasma to rituximab for the treatment of patients with refractory advanced CLL. *QJM* 2008; **101**: 737–740.
- Tedesco F, Bulla B, Fischetti F. Terminal complement complex: regulation of formation and pathophysiological function. In: Szebeni J (ed). *The Complement System: Novel Rules in Health and Disease*. pp 97–127, 2004.
- Garred P, Hetland G, Mollnes TE, Stoerholdt G. Synthesis of C3, C5, C6, C7, C8, and C9 by human fibroblasts. *Scand J Immunol* 1990; **32**: 555–560.
- Langegegen H, Pausa M, Johnson E, Casarsa C, Tedesco F. The endothelium is an extrahepatic site of synthesis of the seventh component of the complement system. *Clin Exp Immunol* 2000; **121**: 69–76.
- Langegegen H, Berge KE, Macor P, Fischetti F, Tedesco F, Hetland G *et al*. Detection of mRNA for the terminal complement components C5, C6, C8 and C9 in human umbilical vein endothelial cells *in vitro*. *APMIS* 2001; **109**: 73–78.
- Gelderman KA, Tomlinson S, Ross GD, Gorter A. Complement function in mAb-mediated cancer immunotherapy. *Trends Immunol* 2004; **25**: 158–164.
- Fishelson Z, Donin N, Zell S, Schultz S, Kirschfink M. Obstacles to cancer immunotherapy: expression of membrane complement regulatory proteins (mCRPs) in tumors. *Mol Immunol* 2003; **40**: 109–123.
- Ziller F, Macor P, Bulla R, Sblattero D, Marzari R, Tedesco F. Controlling complement resistance in cancer by using human monoclonal antibodies that neutralize complement-regulatory proteins CD55 and CD59. *Eur J Immunol* 2005; **35**: 2175–2183.
- Macor P, Tripodo C, Zorzet S, Piovani E, Bossi F, Marzari R *et al*. *In vivo* targeting of human neutralizing antibodies against CD55 and CD59 to lymphoma cells increases the antitumor activity of rituximab. *Cancer Res* 2007; **67**: 10556–10563.
- Golay J, Manganini M, Facchinetti V, Gramigna R, Broady R, Borleri G *et al*. Rituximab-mediated antibody-dependent cellular cytotoxicity against neoplastic B cells is stimulated strongly by interleukin-2. *Haematologica* 2003; **88**: 1002–1012.
- Golay J, Zaffaroni L, Vaccari T, Lazzari M, Borleri GM, Bernasconi S *et al*. Biologic response of B lymphoma cells to anti-CD20 monoclonal antibody rituximab *in vitro*: CD55 and CD59 regulate complement-mediated cell lysis. *Blood* 2000; **95**: 3900–3908.
- Di Gaetano N, Cittera E, Nota R, Vecchi A, Grieco V, Scanziani E *et al*. Complement activation determines the therapeutic activity of rituximab *in vivo*. *J Immunol* 2003; **171**: 1581–1587.
- Di Niro R, Ziller F, Florian F, Crovella S, Stebel M, Bestagno M *et al*. Construction of miniantibodies for the *in vivo* study of human autoimmune diseases in animal models. *BMC Biotechnol* 2007; **7**: 46.
- Fang J, Qian JJ, Yi S, Harding TC, Tu GH, VanRoey M *et al*. Stable antibody expression at therapeutic levels using the 2A peptide. *Nat Biotechnol* 2005; **23**: 584–590.
- Hanke T, Szawlowski P, Randall RE. Construction of solid matrix-antibody-antigen complexes containing simian immunodeficiency virus p27 using tag-specific monoclonal antibody and tag-linked antigen. *J Gen Virol* 1992; **73**(Pt 3): 653–660.
- Boscolo S, Mion F, Licciulli M, Macor P, De Maso L, Brce M *et al*. Simple scale-up of recombinant antibody production using an UCOE containing vector. *N Biotechnol* 2012; **29**: 477–484.
- Macor P, Mezzanzanica D, Cossetti C, Alberti P, Figini M, Canevari S *et al*. Complement activated by chimeric anti-folate receptor antibodies is an efficient effector system to control ovarian carcinoma. *Cancer Res* 2006; **66**: 3876–3883.

- 42 Mezzaroba N, Zorzet S, Secco E, Biffi S, Tripodo C, Calvaruso M *et al.* New potential therapeutic approach for the treatment of B-Cell malignancies using chlorambucil/hydroxychloroquine-loaded anti-CD20 nanoparticles. *PLoS One* 2013; **8**: e74216.
- 43 Biffi S, Garrovo C, Macor P, Tripodo C, Zorzet S, Secco E *et al.* *In vivo* biodistribution and lifetime analysis of cy5.5-conjugated rituximab in mice bearing lymphoid tumor xenograft using time-domain near-infrared optical imaging. *Mol Imaging* 2008; **7**: 272–282.
- 44 Biffi S, Dal Monego S, Dullin C, Garrovo C, Bosnjak B, Licha K *et al.* Dendritic polyglycerolsulfate near infrared fluorescent (NIRF) dye conjugate for non-invasively monitoring of inflammation in an allergic asthma mouse model. *PLoS One* 2013; **8**: e57150.
- 45 Ridgway JB, Presta LG, Carter P. ‘Knobs-into-holes’ engineering of antibody CH3 domains for heavy chain heterodimerization. *Protein Eng* 1996; **9**: 617–621.
- 46 Reed CD, Rast H, Hu WG, Mah D, Nagata L, Masri SA. Expression of furin-linked Fab fragments against anthrax toxin in a single mammalian expression vector. *Protein Expr Purif* 2007; **54**: 261–266.
- 47 Funakoshi S, Longo DL, Murphy WJ. Differential *in vitro* and *in vivo* antitumor effects mediated by anti-CD40 and anti-CD20 monoclonal antibodies against human B-cell lymphomas. *J Immunother Emphasis Tumor Immunol* 1996; **19**: 93–101.
- 48 Cragg MS, Morgan SM, Chan HT, Morgan BP, Filatov AV, Johnson PW *et al.* Complement-mediated lysis by anti-CD20 mAb correlates with segregation into lipid rafts. *Blood* 2003; **101**: 1045–1052.
- 49 Cragg MS, Glennie MJ. Antibody specificity controls *in vivo* effector mechanisms of anti-CD20 reagents. *Blood* 2004; **103**: 2738–2743.
- 50 Gunn L, Ding C, Liu M, Ma Y, Qi C, Cai Y *et al.* Opposing roles for complement component C5a in tumor progression and the tumor microenvironment. *J Immunol* 2012; **189**: 2985–2994.
- 51 Dobrina A, Pausa M, Fischetti F, Bulla R, Vecile E, Ferrero E *et al.* Cytolytically inactive terminal complement complex causes transendothelial migration of polymorphonuclear leukocytes *in vitro* and *in vivo*. *Blood* 2002; **99**: 185–192.
- 52 Markiewski MM, DeAngelis RA, Benencia F, Ricklin-Lichtsteiner SK, Koutoulaki A, Gerard C *et al.* Modulation of the antitumor immune response by complement. *Nat Immunol* 2008; **9**: 1225–1235.